

Experimental Investigation of Dynamics and Atomization of a Liquid Film Flowing over a Spinning Disk

M. Freystein, T. Gambaryan-Roisman^{1,2,*}, P. Stephan^{1,2}

¹Institute of Technical Thermodynamics, Technische Universität Darmstadt, Darmstadt, Germany

²Center of Smart Interfaces, Technische Universität Darmstadt, Darmstadt, Germany
freystein@ttd.tu-darmstadt.de, gtatiana@ttd.tu-darmstadt.de, pstephan@ttd.tu-darmstadt.de

Abstract

One of the most commonly used methods of liquid atomization is the rotary atomization. In this process a radially spreading thin liquid film is created on a surface of a rotating disk, due to centrifugal forces. The liquid flows over the disk edge and disintegrates. The liquid film is mostly wavy. The radially propagating waves induce fluctuations resulting in an expansion of the drop size distribution after atomization.

A new experimental apparatus has been built to investigate the effect of the film dynamics on the atomization process. A water jet is impinging at the center of a rotating disk made of stainless steel. The local instantaneous film thickness is measured using a confocal chromatic sensing technique. The drop sizes are determined using the shadowgraphy method. The film flow on the rotating disk has been investigated in a wide range of parameters. The strongly wavy structure of the film flow has been observed for all sets of parameters. The development of waves depends on the nozzle-to-disk distance. The radial distribution of the time-averaged film thickness over the disk surface agrees fairly well with the correlations found in the literature. First results of the drop size distribution show a bimodal distribution for low mass flow rates.

Introduction

Many intermediate and final products in chemical, pharmaceutical and food industry and in material processing are in the form of powder. The production of powder in spray processes is very common in industrial applications [1, 2]. The requirements to the powder products, depending on their application, concern the particle size, shape, composition, density and chemical properties. Usually a narrow distribution of the powder particles is desirable. The properties of the particles are determined by the size and composition of the droplets in the spray and by the heat and mass transport between the droplets and the environmental gas.

In spray drying, rotary atomizers are frequently used for the spray formation [3]. In this technique a thin liquid film is formed and spreads over a spinning disk. In most of the cases the film is wavy. As the film flows over the disk edge, it disintegrates into droplets forming a spray. The influence of the liquid film hydrodynamics on the spray characteristics is not yet completely understood.

The gas-liquid interface of a film flowing over a rotating disk is in the most cases wavy [4 – 7]. The flow waviness enhances the heat and mass transfer and has a potential as a process intensification technique when performing gas/liquid/solid contacting operations [8]. However, the waviness of the film flow has disadvantages for atomization processes. The radial propagating waves are inducing fluctuations and these fluctuations are influencing the drop size and resulting in an expansion of the drop size distribution. The control and stabilization of the film flow on rotating disks is important for the improvement of the atomization technology.

The hydrodynamics of films flowing over rotating disk has been studied theoretically, numerically and experimentally. An early theoretical investigation of spinning disk atomization has been performed by Bär [9]. Based on the assumption of a laminar waveless flow and taking into account the balance between the viscous and the centrifugal force, he derived an expression for the film thickness as a function of the distance from the disk center. This expression is applicable far from the disk center.

Theissing [10] has performed a numerical simulation of the waveless film flow over a rotating disk using the boundary layer-type equations. During the last decade the problem of film flow over a rotating disk has been treated in the framework of the integral boundary layer method [6, 11, 12]. The application of this method allows examination of the wave regimes [6, 12] on the liquid-gas interface and investigation of the effects of disk topography and of the flow rate modulation on the film dynamics.

Several experimental methods for determination of the film thickness have been applied to investigate the film flow on a rotating disk, including needle method [4, 8], electrical resistance method [13], capacitance method [14] and infrared absorption [5]. Due to limitations in temporal resolution or spatial resolution so far most of

*Corresponding Author: gtatiana@ttd.tu-darmstadt.de

the experimental studies dealt with the determination of the time- and spatially-average film thickness. Of all of the methods mentioned above, only the needle method allows measurement over the entire disk radius [15].

In this work, a new experimental apparatus for a combined measurement of drop size distribution and film evolution on a rotating disk has been developed. The used confocal chromatic sensing technique (CHR) for the measurement of liquid film thickness has significant advantages compared to the above mentioned measurement techniques. The method allows the measurement of the local film thickness with a high temporal resolution of 4 kHz. Apart from that, the distribution of the film thickness over nearly the entire disk radius can be measured. The CHR technique has been used for determination of the spatial distribution of the time-averaged film thickness in a wide range of experimental parameters and for characterization of the waves on the liquid-gas interface. The droplets created at the edge of the disk have been characterized using the shadowgraphy method.

Experimental Setup and Measurement Instrumentation

The experimental setup consists of the test section with the rotating disk (radius $r_d = 7.5 \cdot 10^{-2}$ m) and a fluid loop. The flow chart of the experimental setup is shown in Fig. 1. All tests have been carried out at ambient pressure conditions of 1 bar. Deionized water has been used as a test liquid. The liquid is pumped from a reservoir by a progressive cavity pump (1), which produces only very small vibrations into the flow. Using three different interchangeable eccentric screws, the mass flow rate can be varied in a wide range 2 – 400 kg/h. The water temperature at the nozzle inlet is kept constant at $t_{in} = 20^\circ\text{C}$. After the Coriolis flow meter (2) the fluid enters the nozzle which is positioned centrally above the disk. Different solid stream nozzles have been used with diameters ranging from $d_n = 0.34$ mm to $d_n = 3.4$ mm. The liquid jet out of the nozzle impinges at the center of the rotating disk. The liquid, which is accelerated by the centrifugal force, spreads over the rotating disk and is atomized over the edge of the disk. The droplets are collected in a square cut tray with a lateral length of 1.2 m, and the liquid is led back to the reservoir. The side walls of the tray are made of plexiglass for additional optical access. The distance between the nozzles and the disk can be varied continuously using a linear slide. The disk which has a thickness of 8 mm is manufactured out of stainless steel. The disk upper surface is polished. A chamfer is machined at the edge of the rotating disk for better atomization behaviour [16]. The rotating disk is connected with a stainless steel drive shaft by heat shrinking. The rotational speed of the disk can be varied in a wide range, whereas two different electrical motors are used for the frequency range $f = 10 - 60$ Hz and $f = 0 - 10$ Hz.

A schematic of the measurement equipment integrated in the test section is shown in Fig. 2. The wavy patterns at the liquid-gas interface are observed using a high-speed b/w camera. The local and temporal film thickness is measured using a confocal chromatic sensing (CHR) technique, which is based on chromatic longitudinal aberration of special optical probe [17]. The white light of a halogen lamp is coupled into an optical fiber and led to the detector head positioned vertically above the disk. Due to the special optical probe the focal length is depending on the wavelength. Using a spectrometer the reflected light is analysed and a sharp peak is visible for the wavelength focussed on the film surface. For thickness measurements a second sharp peak of the reflecting light is visible for the wall surface. Knowing the refraction index of the fluid the distance between the two peaks allows the conclusion about the film thickness. This technique has a measurement error for the film thickness of less than 5 μm . The size of the measurement spot depends on the sensor type and varies between 2 μm for a measurement range of about 150-200 μm and 16 μm for film thicknesses up to 3,000 μm . The detector head is positioned above the disk and the measurement position can be varied radial in micrometre steps from $r = 32$ mm to the edge of the disk using a linear slide. The film thickness has been measured with a frequency of 4 kHz. The presented average film thicknesses are averaged over a period of ten seconds.

The atomization process of the liquid film has been characterized using a high-speed b/w camera and a vertically aligned light source. Close to the edge of the disk the disintegration of the liquid can be observed. The drop sizes have been determined using a shadowgraphy technique. The images of the drops have been processed using an inhouse algorithm. For each of the captured drops the average drop diameter has been calculated as the arithmetic average of maximal lengths in two orthogonal spatial directions. In order to cover different orders of magnitude of droplet sizes, different lenses have been used. The highest lens resolution was 2.5 $\mu\text{m}/\text{pixel}$.

Data Analysis

The experimental results on the time-averaged film thickness measurements have been compared with correlations found in literature. Following the approach developed in [9, 10], we define dimensionless radial coordinate and dimensionless film thickness by the following expressions:

$$r^* = r \left(\frac{2\pi}{V} \right)^{1/2} (\nu\omega)^{1/4}, \quad (1)$$

$$\delta^* = \delta(\nu/\omega)^{-1/2}, \quad (2)$$

where \dot{V} denotes the volume flow rate of the liquid, ν is the kinematic viscosity of the fluid, r is the radial position, ω is the angular velocity of the disk rotation and δ the film thickness.

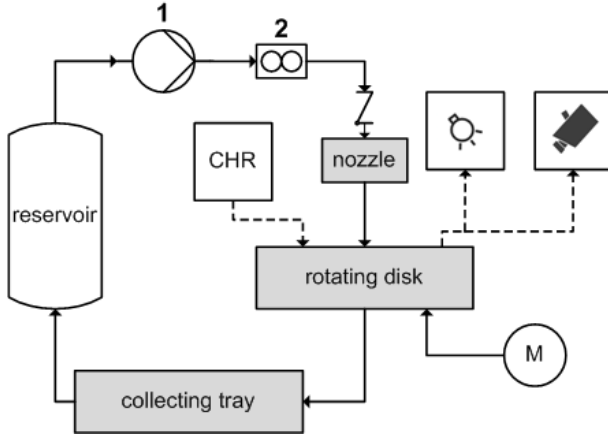


Figure 1 Schematic of experimental loop.

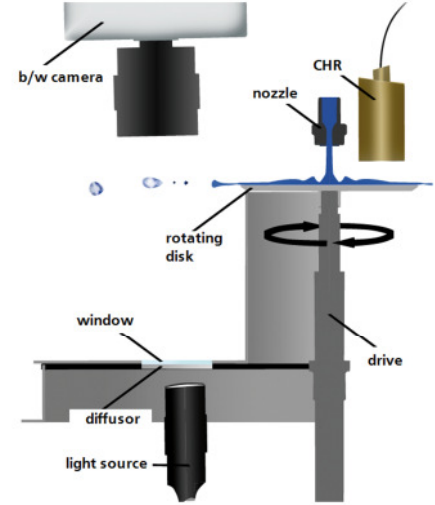


Figure 2 Schematic of measurement equipment.

In the case of a laminar and waveless film flow and under the assumption that the film hydrodynamics are dominated by the viscous and centrifugal forces the film thickness can be determined from the following equation [9]:

$$\delta = \left(\frac{3 \dot{V} \nu}{2 \pi r^2 \omega^2} \right)^{1/3} \quad (3)$$

The applicability region of this relation has been estimated in different works as $r^* > 2$ [18], or $r^* > 1$ [10]. For smaller radial positions, where inertial effects significantly affect the film hydrodynamics, Eq. (3) is not applicable.

Theissing [10] has determined the film thickness in a wide range of r^* values by numerical integration of boundary layer-like equations. He has developed a correlation for δ^* on the basis of numerical solution. The effect of the inlet conditions is described in terms of a dimensionless inlet number H^* :

$$H^* \equiv \frac{0.5 v_n^2 + g h}{\omega^{1.5} \dot{V} \eta^{-0.5} \rho^{0.5}} \quad (4)$$

where v_n is the velocity at the nozzle exit, g denotes the gravitational acceleration, h is the distance between the nozzle and the disk, η and ρ are the dynamic viscosity and the density of the liquid, respectively. The dimensionless radial velocity of the liquid, averaged over the film thickness, v_r^* , is correlated using the parameters v_i^* and v_a^* and a weighting factor Y :

$$v_i^* = (2 H^*)^{0.5} \quad (5)$$

$$v_a^* = \frac{0.204}{r^{*1/3} \left(1 + \frac{1.14}{r^{*8}} \right)^{1/6}} \quad (6)$$

$$Y = \frac{1}{\left(1 + \frac{1}{17.5 r^{*6.2}} \left(1 + \left(\frac{1.8 H^{*0.5}}{r^*} \right)^{5/3} \right)^{-3/5} \right)^{1/5}} \quad (7)$$

$$v_r^* = (1 - Y) v_i^* + Y v_a^* \quad (8)$$

The dimensionless film thickness δ^* can be calculated using the mass balance relation:

$$\delta^* = \frac{1}{2\pi r^* v_r^*} \quad (9)$$

For large values of the dimensionless radius r^* the correlation given by Eqs.(4 – 9) coincides with the asymptotic solution(3). It has to be noted that in the original publication [9] Eq. (7) contains a typing error. An exponent ‘0.2’ is typed instead of ‘6.2’. The correlation (4-9) is characterized by a present of a maximum of the film thickness at a certain dimensionless distance from the disk centre.

In our work the film thickness distribution in the whole range of experimental parameters has been compared with the correlation (4 – 9).

Results and Discussion

The film thickness distribution has been recorded for the range of the liquid mass flow rate 25 kg/h to 150 kg/h and for rotational speeds up to 600 rpm. The experimental reproducibility is very good, as illustrated in Fig. 3.

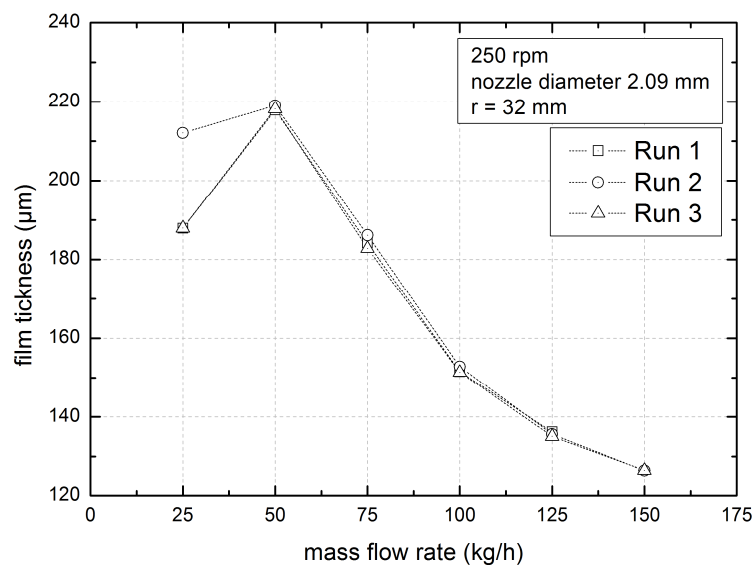


Figure 3 Results of three test series for the time-averaged film thickness as a function of mass flow rate for a radial position of $r = 32$ mm and a rotational speed of 250 min^{-1} .

The experimental data on the time-averaged film thickness has shown a very good reproducibility for different radial measurement positions and different rotational speeds. The only exception is the film thickness value at the smallest mass flow rate of 25 kg/h. The poor reproducibility of the film thickness data at the mass flow rate of 25 kg/h is caused by a partial dryout of the disk surface. A necessary minimum mass flow rate for complete wetting of the disk surface is not reached at this flow rate [19]. Random wet and dry parts of the disk are alternating below the sensor due to the disk rotation, which leads to a large scatter of the film thickness data between different test series. In Fig. 4 the local instantaneous film thickness evolution for a mass flow rate of 75 kg/h and three different values of rotational speed is shown. The strongly wavy pattern of the film can be clearly observed. Apart from the decrease of the average film thickness with increasing rotational speed, no influence of rotational speed on the film dynamics is visible. The evaluation of instantaneous film thickness data at different radial positions confirms that there is no clear dependency between the rotational speed and the characteristics of the wavy film structure.

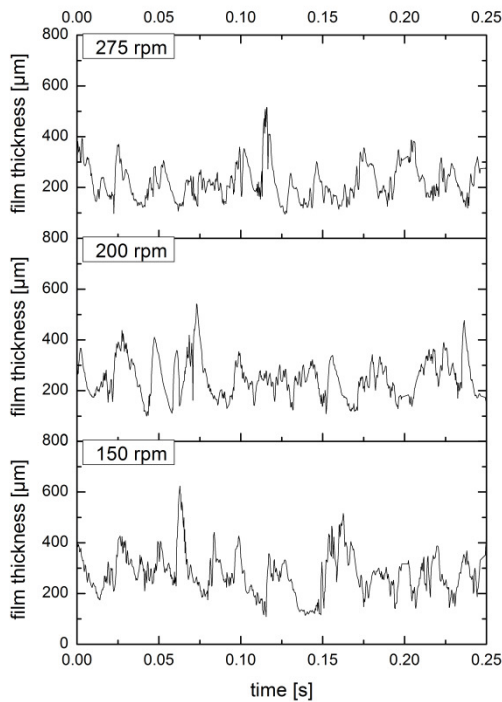


Figure 4 Local film thickness at a radial position of $r = 55$ mm for a mass flow rate of 75 kg/h and three different rotational speeds (distance between nozzle and disk $h = 5$ mm).

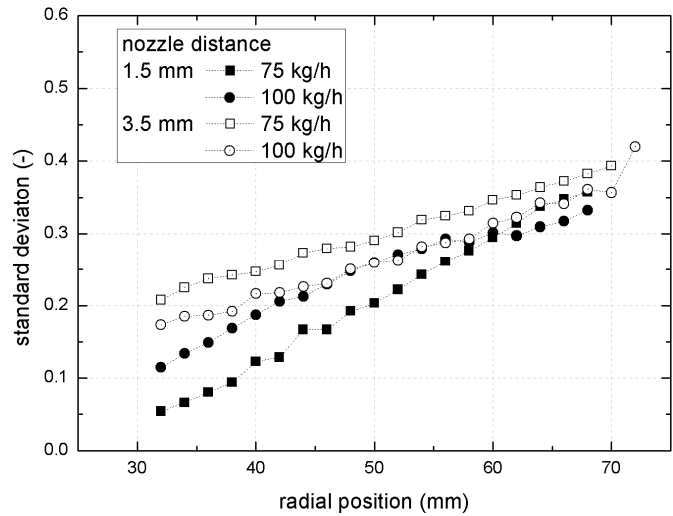


Figure 5 Standard deviation from time-averaged film thickness at a radial position of $r = 32$ mm and a rotational speed of 250 min^{-1} for two different nozzle-to-disk distances.

The influence of the distance between the nozzle and the rotating disk on the characteristics of the wavy motion is illustrated in Fig. 5. The standard deviation of the instantaneous film thickness from the time-averaged thickness is normalized by dividing through the local average film thickness. This parameter, which correlates with the characteristic amplitude of the waves, is represented as a function of radial position. It can be observed that the standard deviation of the film thickness increases with increasing of the distance from the disk center. Close to the impinging jet the high-speed imaging of the liquid-gas interface shows axisymmetric radial waves that are disintegrating into three-dimensional wave structures at a certain distance from the disk centre.

Figure 5 shows that the standard deviation of the film thickness depends on the distance between the nozzle and the disk surface. Close to the centre of the disk the film waviness can be significantly reduced by shortening the distance between the nozzle and the rotating disk. For a mass flow rate of 75 kg/h no waves can be observed at the measurement position closest to the disk center. With increasing radial position the difference of wave characteristics between the experiments performed with the nozzle-to-disk distance of 1.5 mm and 3.5 mm becomes smaller. The effect of the nozzle-to-disk distance on the wavy pattern in the vicinity of the disk center can be attributed to the capillary instability of the jet leading to a periodic modulation of the mass flow rate of the impinging jet.

In Fig. 6 radial profiles of the time-averaged film thickness are shown for six different mass flow rates. The position of the CHR-sensor has been varied during the experiment in equally spaced steps of 2 mm using a linear slide. For the smallest flow rate of 25 kg/h a continuous decrease of the time-averaged film thickness can be seen. The film flow on the rotating disk is dominated by the centrifugal force. An increase in mass flow rate leads to a qualitative change of the profile. An increase up to a maximum and afterwards a continuous decrease of the film thickness can be observed with increasing r . For higher mass flow rates this maximum is shifted towards higher radii, but the maximal time-averaged film thickness remains a constant value of about $\delta \approx 225$ mm. Since the nozzle diameter has been kept constant at $d_n = 2.09$ mm, the jet velocity drastically increases with increasing of the mass flow rate. This explains the shift of the maximum film thickness towards larger values of r and a reduction of the region where the flow is dominated by the viscosity and centrifugal force only.

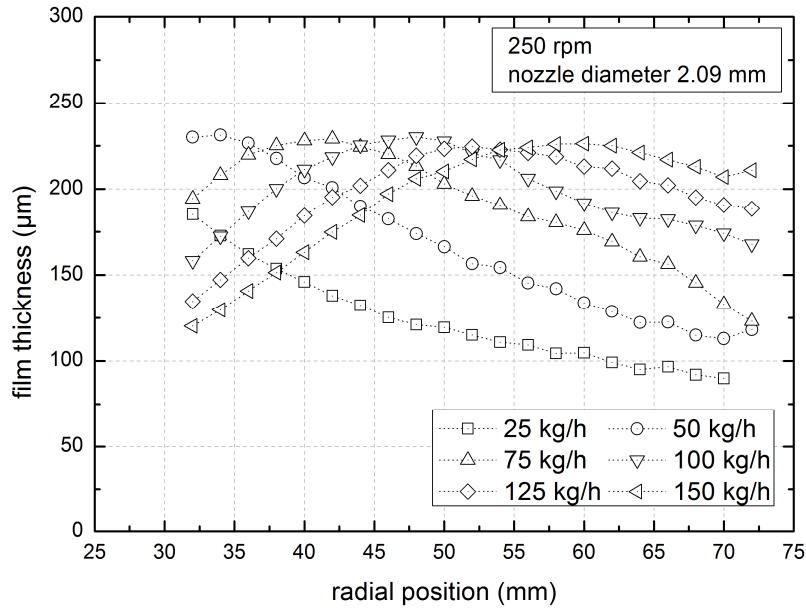


Figure 6 Average film thickness as a function of radial position for a rotational speed of 250 min^{-1} and a variation of mass flow rates

In Fig. 7 the comparison between the experimental data and the correlations from the literature is shown. For $r^* > 1$ the experimental results are in a fairly good agreement with the asymptotic solution (3). Equation (3) only slightly overpredicts the film thickness. It is notable that nearly the whole distribution of the time-averaged film thickness agrees fairly well with the correlation (4-5). The position and the value of the film thickness maximum are excellently predicted.

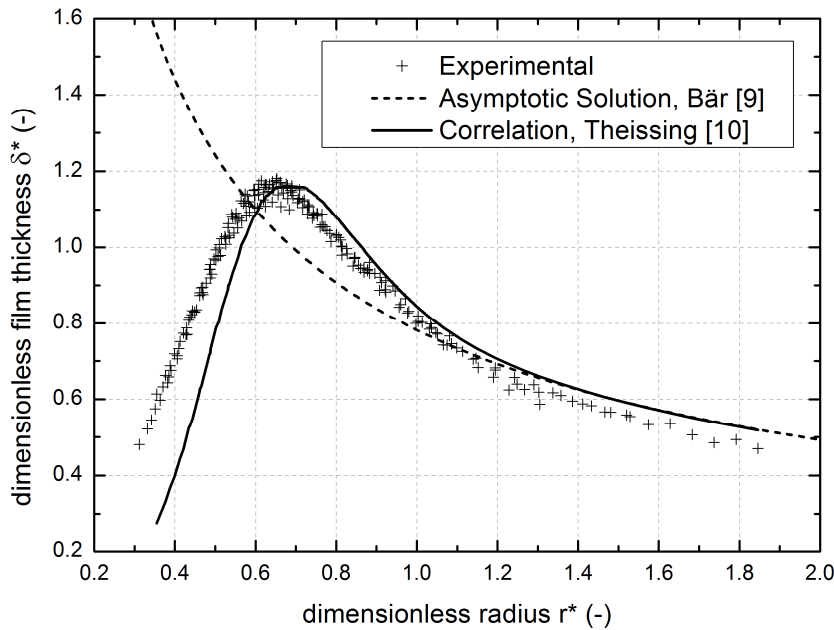


Figure 7 Dimensionless film thickness δ^* as a function of the dimensionless radius r^* for a variation of mass flow rates (25 – 150 kg/h) and rotational speed (100 – 300 rpm) and comparison with correlations of literature

First experimental results on the drop size distribution are shown in Fig. 8. In this image, a normalized sum distribution of the drop sizes is presented for a mass flow rate of 25 kg/h and for several values of the rotational speed. A plateau in this graph indicates a range of diameters in which no drops are present. For decreasing rotational speeds the drop size distribution is expanding as expected. Apart from the expansion, an additional effect could be observed. As the rotational speed of the disk decreases, the drop distribution becomes bimodal while the minimum drop size diameter is independent from the rotational speed.

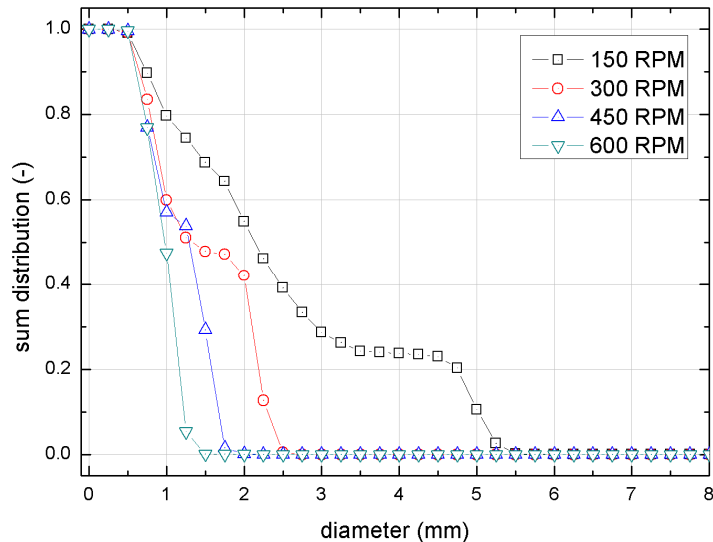


Figure 8 Normalized sum distribution for a mass flow rate of 25 kg/h and a variation of rotational speed

Although the exact correlation between the film hydrodynamics and the droplet size distribution has not yet been established, it can be supposed that the film waviness is responsible for the formation of sprays with wide distribution of the drop sizes. In previous studies it has been already reported that longitudinal grooves on the surface are significantly stabilizing the flow of liquid falling films [20, 21]. Since the physical mechanisms governing the falling film flow and the flow of films over rotating discs are rather similar, it can be expected that the longitudinal grooves may suppress the development of waves in liquid films flowing along rotating disks. Our future works will be aimed at controlling the wavy structure of the liquid film by using a structured disk surface, which is expected to improve the drop size distribution.

Summary and Conclusions

The dynamics of a thin water film flowing over a rotating disk has been studied using a confocal chromatic sensing technique and high-speed imaging. The radial average film thickness profiles as well as the local instantaneous film thickness have been measured for a wide range of parameters.

It has been found that the rotational speed and the mass flow rate have no distinctive influence on the waviness of the film flow. The wave formation could be suppressed by reducing the distance between the nozzle and the disk surface. The effect of the nozzle-to-disk distance on the wave characteristics is strong for small radial positions and is diminishing towards the edge of the disk.

At low mass flow rates the film thickness continuously decreases with increasing distance from the disk center, which indicates that the flow is dominated by viscosity and centrifugal force. At higher mass flow rates a maximum of the film thickness can be observed on the film thickness profile.

The comparison with correlations from literature shows a quantitatively good agreement for large dimensionless radii but only a qualitative good agreement for moderate values. First experimental results on the drop size distributions show the development of bimodal distribution for small mass flow rates of the impinging liquid within the experimental range of parameters.

Acknowledgements

The authors wish to acknowledge the support of the German Science Foundation, DFG, through the project GA 736/4-1.

References

- [1] Lefebvre, A.H., Atomization and sprays, Hemisphere Publishing Cooperation, Washington, DC. (1989)
- [2] Nasr, G.G., Yule, A.J., Bendig L., Industrial sprays and atomization: Design, analysis and atomization, Springer, London (2002)
- [3] Schroeder, T., Walzel, P., Design of laminar operating rotary atomizers under consideration of the detachment geometry, Chemical Engineering Technology 21(4): 349-354 (1998)
- [4] Espig, H., Hoyle, R., Waves in a Thin Liquid Layer on a Rotating Disc, J. Fluid Mech. 4: 671-677 (1965)
- [5] Charwat, A.F., Kelly, R.E., Gazley, C., The Flow and Stability of Thin Liquid Films on a Rotating Disk, J. Fluid Mech. 53: 227-255 (1972)
- [6] Sisoiev, G.M., Matar, O.K., Lawrence, C.J., Axisymmetric Wave Regimes in Viscous Liquid Film Flow over a Spinning Disc, J. Fluid Mech. 495: 385-411 (2003)

- [7] Woods, W., The hydrodynamics of thin liquid films flowing over a rotating disc, Ph.D. thesis, Newcastle University (1995)
- [8] Aoune, A., Ramshaw, C., Process Intensification: heat and mass transfer characteristics of liquid films on rotating discs, *International Journal of Heat and Mass Transfer* 42: 2543-2556 (1999)
- [9] Bär, P., Über die physikalischen Grundlagen der Zerstäubungstrocknung, PhD Thesis, TH Karlsruhe, Germany (1935)
- [10] Theissing, P., Erzeugung von Flüssigkeitsfilmen, Flüssigkeitslamellen und Tropfen durch rotierende Scheiben, PhD Thesis, TU Berlin, Germany (1975)
- [11] Matar, O.K., Sisoiev, G.M., Lawrence, C.J., The flow of thin liquid films over spinning discs, *The Canadian Journal of Chemical Engineering* 84: 625-642 (2006)
- [12] Sisoiev, G.M., Goldgof, D.B., Korzhova, V.N., Stationary Spiral Waves in Film Flow over a Spinning Disk, *Phys. Fluids* 22:052106 (2010)
- [13] Miyasaka, Y., On the flow of a viscous free boundary jet on a rotating disk, *Bull. JSME* 17: 1469-1475 (1974)
- [14] Thomas, S., Faghri, A., Hankey, W., Experimental analysis and flow visualization of a thin liquid film on a stationary and rotating disk, *Journal of Fluids Engineering* 113: 73-80 (1991)
- [15] Leshev, I., Peev, G., Film flow on a horizontal disk, *Chemical Engineering and Processing* 42: 925-929 (2002)
- [16] Frost A.R., Rotary Atomization in the Ligament Formation Mode, *Journal of agric. Engineering Research* 26: 63-78 (1981)
- [17] Kunkel, M., Schulze, J., Mittendicke von Linsen beruehrungslos messen, *Photonik*, no. 6 (2004)
- [18] Brauer, H., Grundlagen der Einphasen- und Mehrphasenströmung, Sauerländer Verlag, Germany (1971)
- [19] Wozniak, G., Zerstäubungstechnik, Springer, Germany (2003)
- [20] Gambaryan-Roisman, T., Stephan, P., Analysis of Falling Film Evaporation on Grooved Surfaces, *International Journal of Enhanced Heat Transfer* 10: 445-457 (2003)
- [21] Helbig, K., Nasarek, R., Gambaryan-Roisman, T., Stephan, P., Effect of Longitudinal Mini-Grooves on Flow Stability and Wave Characteristics of Falling Liquid Films, *ASME Journal of Heat Transfer* 131:011601 (2009)